Hindawi
Geofluids
Volume 2022, Article ID 9735532, 10 pages
https://doi.org/10.1155/2022/9735532

Research Article

Model Test of TBM Tunnel Crossing Large Dip Angle Fault Zone under High In Situ Stress

Liming Wang[1,2] **Kairong Hong**,[1,2] **Yongwei Quan**,[3] **Hailei Zhao**[1,2] **Xiangbo Zhao**,[3] **Zhenxing Yang**,[1,2] **and Zhenliang Zhou**[4]

[1]*State Key Laboratory of Shield Machine and Boring Technology, Zhengzhou 450001, China*
[2]*China Railway Tunnel Group Co., Ltd., Guangzhou 511458, China*
[3]*Xinjiang Erqis River Investment Development (Group) Co., Ltd., Urumqi 830000, China*
[4]*Beijing Jiaotong University, Beijing 100000, China*

Correspondence should be addressed to Hailei Zhao; zhaohailei3@crecg.com

Received 23 June 2022; Revised 29 July 2022; Accepted 12 August 2022; Published 12 September 2022

Academic Editor: Zhengzheng Xie

In order to study the effect of fracture zone on tunnel stability under high ground stress and to reveal the disaster mechanism of fracture zone surrounding rock compressor, the TBM tunnel of Fragrant Furnace Mountain Tunnel in the F12 fracture zone in Dali I section of central Yunnan was experimentally studied. The results show that the TBM cutter head has a significant effect on the surrounding rock pressure in the range of 0.43 D~0.5 D (hole diameter), with a maximum increase of 1.19-fold. As the measurement point approaches the tunnel contour, the displacement of surrounding rock increases. As TBM traverses the fracture zone interface, the displacement of surrounding rock increases at the maximum rate. The effect of TBM shear rock formation failure on the internal displacement of rock formation is 1.21 D in the front and not more than 1.5 D in the top. Sliding and loosening of the fault zone looser above the interface can easily lead to blockage of the fault zone, and the pressure of the surrounding rocks at front edge does not affect more than 1.73 H (the length of horizontal projection of the fault zone interface). Therefore, in the course of construction, the interface of fracture zone should be promoted to reduce the construction risks.

1. Introduction

With the development of the world economy, TBM tunnels in transportation and water conservancy construction are developing in the direction of "long, large, deep, and swarm" [1–4]. In the construction of deep-buried long tunnels, there are often extremely complicated geological conditions such as high ground stress, large deformation of soft rock, and fault zone. Therefore, in the course of TBM construction, the adhesive machine has great risks and brings great challenges to construction [5–8]. Stress redistribution rock deformation and tunnel instability are closely related to time and construction technology during TBM stress redistribution tunneling. It is important to master the rules of mechanical effect in tunnel construction to guide the design and tunnel construction of tunnel [9–13].

Numerical simulation, model test, and field test are often used to study the mechanical effects of TBM across fault zones. In terms of numerical simulation, Liu et al. [14] established a three-dimensional numerical model for the construction condition of open TBM crossing the fault fracture zone and studied the variation rule of TBM cutter head, shield structure, and initial support force. Maleki and Dehnavi [15] analyzed the deformation law of surrounding rock when TBM traverses the compressive fracture zone through FLAC and UDEC numerical simulation methods for engineering cases and analyzed the disaster mechanism of TBM stuck machine. Jian-long et al. [16] used FLAC3D

to establish the simulation of TBM tunneling working conditions with double shields, studied the influence of tunnel longitudinal displacement release rate and other factors on tunnel surrounding rock deformation, and revealed the interaction mechanism between TBM and surrounding rock. Chakeri et al. [17], Hasanpour et al. [18], and Lambrughi et al. [19] presented a 3D numerical model using the finite difference code FLAC3D for mechanized excavations, which was capable of simulating a tunnel excavation when an earth pressure balance- (EPB-) TBM was used. In the aspect of the model test, Ketan et al. [20] developed a new experimental device to simulate the support installation process of tunnel boring machine (TBM) excavation and extrusion of clay-rich rock to study the interaction between surrounding rock and extrusion ground. Jeon et al. [21] used reduced-scale tests to investigate the influences of faults, weak planes, and grouting on tunnel stability. Zhang et al. [22] developed a model test system to simulate the construction of a tunnel by the method of up and down steps. The variation rules of seepage pressure, displacement, stress, and outflow of surrounding rock after excavation of fault were studied. According to the Shuangjiangkou Hydropower Station project, Zhu et al. [23] set up a geomechanical model of a tunnel group under high ground stress and studied the displacement characteristics of surrounding rock during tunneling. Li et al. [24] built a large-scale three-dimensional model of horseshoe-shaped tunnel and analyzed the deformation and failure law of tunnel-fracture rock mass under high stress. Field tests are conducted mainly behind the surface of the tunnel. Ghabraie et al. [25] used several mortar physical models to study the characteristics of multiseam subsidence. The results showed that the panel configurations of the two types of seams have an important influence on the development of multiseam subsidence. Huang et al. [26] carried out field tests on the pressure of surrounding rock, deformation of tunnel, and stress of supporting structure based on tunnel engineering. Zhao et al. [27] carried out field tests on the surrounding rock and initial support structure of TBM tunnel based on KS tunnel of Xinjiang water transmission and studied the mechanical properties of the tunnel support structure.

The numerical simulation method has its limitations due to the small size, composition, and complex geological genesis of TBM equipment and the complicated fault zone conditions. For example, the field test data acquisition lags behind and construction risk are high. The existing model test study on the whole section, mostly artificial excavation tunnel construction simulation, is difficult to fully study TBM tunnel surrounding rock mechanical properties. To greater restore the change law of tunnel surrounding rock when TBM passes through the fault zone in a more limited way, the micro-TBM tunneling comprehensive test platform developed by the State Key Laboratory of Shield and Tunneling Technology was used in this paper to accurately simulate the construction process of TBM tunnel passing through the large dip angle fault zone under high ground and to explore the pressure and deformation failure law of tunnel surrounding rock. It provides a theoretical basis for reducing disaster risk caused by TBM stuck machines.

2. Model Test Principle and Scheme

2.1. Test Principle. This experiment is based on the Xianglushan tunnel project in Dali I of the Central Yunnan Water Diversion Project. The total length of TBM excavation is 20.802 km, and blade diameter is 9.83 m. The average buried depth of the tunnel is about 1200 m, and the in situ stress is high. The tunnel engineering geology condition is complex, and the structure is strongly developed. The whole line crosses 13 faults and active fault zones, among which F12 fault belongs to a regional active large fault, the surrounding rock is V, the width of the fault zone is 165 m, strike NE45, dip NW, dip angle is 60°, and the included angle with the tunnel axis is 68°. The rocks before and after TBM traverse the fault are Mesotriassic North Cliff Group (T_2b^2) limestone, dolomitic limestone, and Permian Emei Shan Formation ($P\beta$) basalt, and the surrounding rock are classified as III2 and III1, respectively. The scale of fault extension is large, and the geomorphic image are clear; the specific structure is shown in Figure 1. Along the fault zone, fault scarps, fault scarps, collapse, landslide, and other undesirable geological phenomena develop. TBM excavation is in high-stress level fault fracture zone, because of the broken surrounding rock and fracture combination cutting; tunnel after excavation is the unstable block, produces the top the arch, slump constant, and falling of deformation such as bending inner drum big; TBM easily trapped card machine, constraints collapse instability, the direction is hard to control, and the TBM support boots failed to move forward the normal construction.

According to similar theory, the experimental platform developed by the State Key Laboratory of Shield Machine and Boring Technology and Excavation Technology is used to simulate the physical and mechanical parameters of the surrounding rock and F12 fault zone. The model test of TBM tunneling through large inclination fault under high ground stress is carried out.

According to the geological survey report of Xianglushan tunnel, the normal surrounding rock mode of the tunnel is configured with similar materials according to type III 2 surrounding rock, the F12 fault zone is configured with similar materials according to type V surrounding rock, and the main physico-mechanical parameters of the surrounding rock of the tunnel are shown in Table 1.

2.2. Similarity Criterion and Similarity Material. The diameter of the TBM cutter head in the xianglushan tunnel is 9.83 m, and the diameter of the miniature TBM cutter head in the test stand is 35 cm. The geometrical similarity ratio of the test is 1 : 28, and the material similarity ratio is 1 : 1. According to the similarity theory, Poisson ratio, friction coefficient ratio is $C_\mu = C_f = 1$, and stress, cohesion, cohesion, and elastic modulus similarity ratio is $C_\sigma = C_{c'} = C_E = 28$.

River sand was used as aggregate cement and gypsum mixture as binder in the surrounding rock of tunnel. Fracture zone chose iron powder, barite powder, and quartz sand as aggregate to be configured into bulk materials, so in this test, we only considered that the fracture zone material has

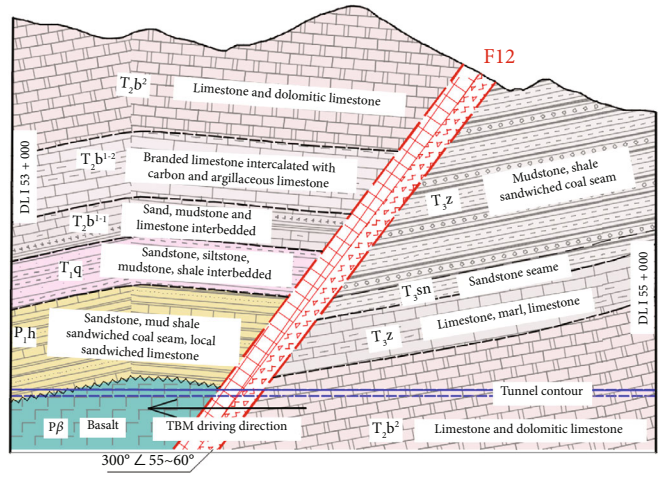

Figure 1: Regional geological profile of the fault zone.

Table 1: Mechanical parameters of prototype and model materials.

Medium	Severe ($kN.m^{-3}$)	Shear strength of rock mass		Poisson's ratio	The compressive strength (MPa)	Modulus of elasticity (GPa)
		f'	c'/(MPa)			
The prototype of the surrounding rock	21.4-27.0	0.8-0.9	0.8-0.9	0.22-0.26	45-55	28.05
Model of the surrounding rock	23.2	0.87	0.03	0.24	1.80	1.00
Fault zone prototype	19.8-22.4	0.45-0.55	0.05-0.1	0.27-0.33	6-8	2.13-23.24
Fault zone model	20.6	/	/	/	/	/
Similar than	1	1	28	1	28	28

(a) Sample making (b) Compression test

Figure 2: Tests on mechanical parameters of similar materials.

a similar mass and internal friction angle, that is, a mass of 20.6 kN/m^3, and the internal friction angle is 28°. Physical and mechanical parameters of other similar materials were measured by indoor tests, as shown in Figure 2.

The mass ratio of similar materials in surrounding rock was determined by repeated experiments to be RS : C : P = 1 : 0.06 : 015 and B : I : S = 1 : 2 : 1.333 in fracture zones, of which RS is river sand, C is cement, P is gypsum, B is barite powder, I iron powder, and S quartz sand. The physical and mechanical parameters of prototype materials and similar materials are shown in Table 1.

2.3. Monitoring Program and Monitoring System. The stress and displacement of surrounding rock in fault zone during excavation of TBM tunneling are studied in this paper. Sensors buried in soil mainly include soil pressure boxes and multipoint displacement meter. Two sections were arranged for the surrounding rock pressure test. The first section of the TBM tunneling direction was 35 mm (0.1 D) above the tunnel vault, with nine earth pressure boxes placed in succession. The second section is perpendicular to the middle of the model, with soil pressure boxes of 0.3 D, 0.5 D, 1 D, and 1.5 D above the vault. The displacement test

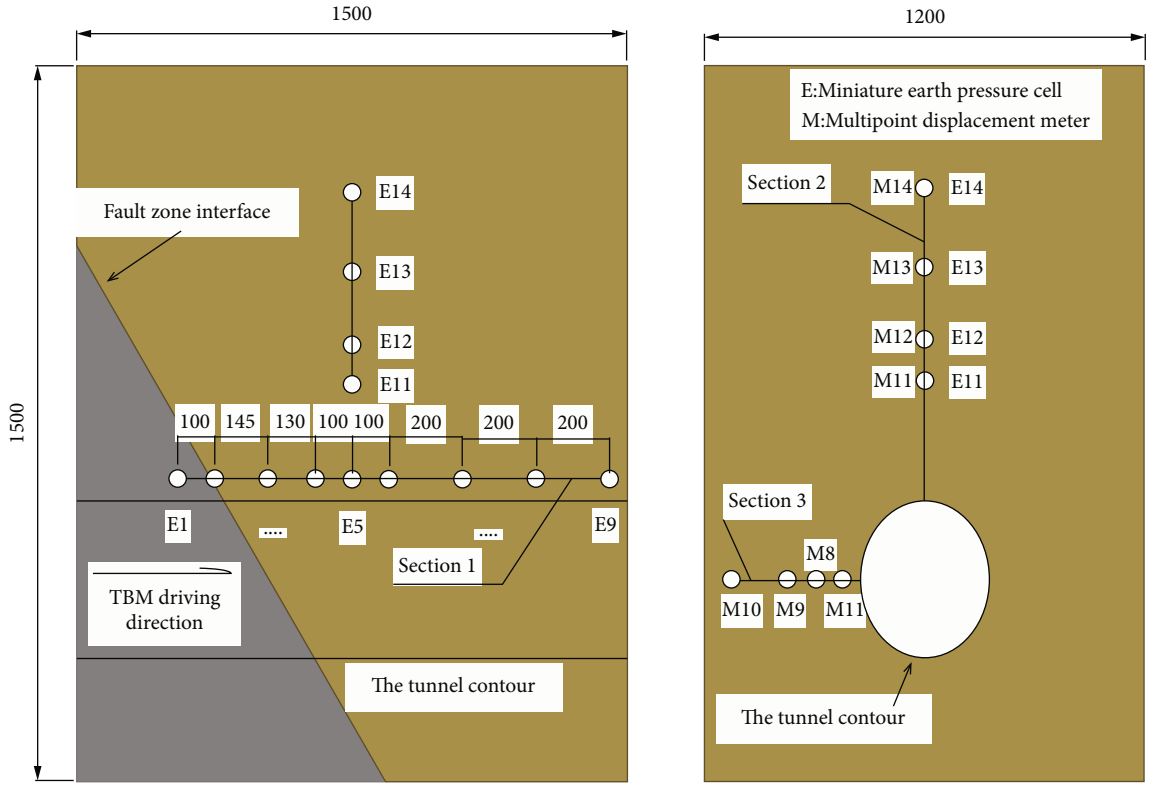

Figure 3: Sensor layout diagram.

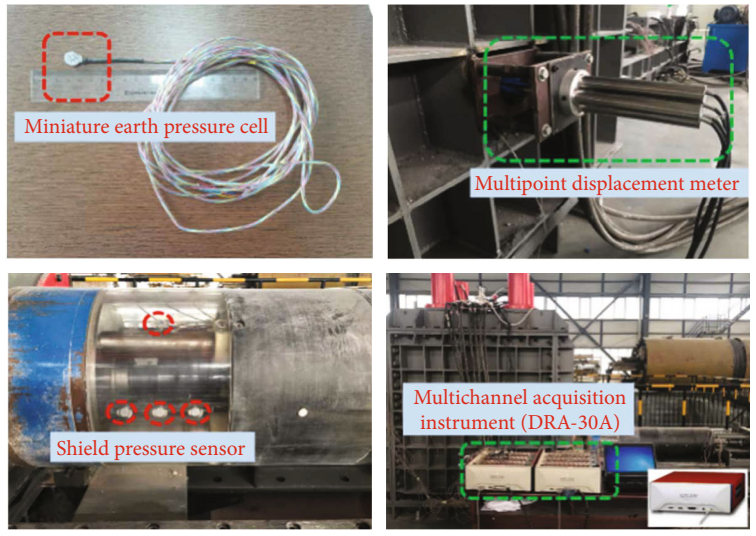

Figure 4: Physical drawing of the multifunctional monitoring system.

of surrounding rock is divided into two sections. In the second section of the pressure test, the vertical displacement is arranged by the earth pressure box, and the horizontal displacement and vertical displacement are vertical. The detailed layout scheme is shown in Figure 3. The DRA-30A multichannel dynamic data acquisition instrument is used for sensor data acquisition at a frequency of once per second and real-time storage. Sensor emplacement and data acquisition are shown in Figure 4.

2.4. Test System and Procedure. The micro-TBM tunneling integrated test bed developed by the State Key Laboratory of Shield Machine and Boring Technology using shield tunneling techniques is shown in Figure 5. The testing platform has the following functions: ① the diameter of micro TBM excavation is 350 mm, and a single excavation forms a tunnel; ② tunneling control system can control the key parameters of TBM tunneling in real-time, and cutter speed can be adjusted in the range of 0-10 r/min, excavating speed

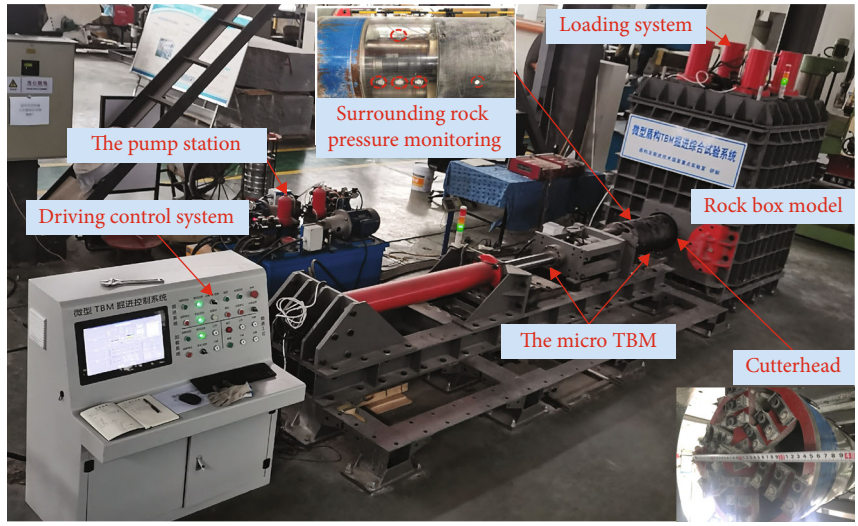

Figure 5: Miniature TBM driving comprehensive test platform.

can be adjusted at 0-50 mm/min, maximum torque is 1300 N.m, maximum thrust is 800 kN, and maximum stroke is 1300 mm; ③ using screw slag system, the speed of slag discharge is adjustable 0-50 r/min, the slag discharge is automatic, and it is convenient to test slag weight; ④ vertical loading system is a quadruple hydraulic system that can be loaded at one point or multiple points. The maximum ground stress of 1.1 MPa can be simulated. ⑤ The box body is welded with Q345 structural steel, and the structural surface is assembled with high strength bolts for easy disassembly. The internal measures 1200 mm × 1500 mm × 1500 mm and has both full and half section excavation functions. The right side can be replaced with a transparent, high-strength glass surface to achieve a micro-TBM semivisible tunnel. Combined with a high-speed camera or digital speckle, it is suitable for the study of the change law and damage form of surrounding rock in tunnel. ⑥ Mini-TBM shield body and L1 area set 1.5 MPa earth pressure box range can monitor shield body and L1 area surrounding rock pressure in real time.

Dimensions of the model are width × length × height = 1200 mm × 1500 mm × 1500 mm with a fault zone inclination angle of 60°. The configured materials are filled by layering compaction, and the specific process is as follows: compounding material according to mass weighting ratio of surrounding rock similar material-mixer mixing evenly-manual layered ramming-sloping to 60° slope-sloping to lay a thin layer of mica powder-mixing material according to mass weighting ratio of fracture zone similar material-mixer mixing evenly-manual layered ramming-sensor wire embedded in design position-sensor wire punched out-filling the remaining material until rock box roof design height.

The TBM excavation was performed under vertical loading during the test. Vertical loading is determined according to design requirements of 1211 m buried depth, and vertical stress reached 1 MPa according to the similarity ratio. The loading steps of the vertical cylinder were 200-400-800-1200-1600-1800 kN, and each stage was static for 2 h. After the load reaches the design value, the excavation test will be started after the stability for 48 h. The entire testing process is shown in Figure 6.

3. Analysis of Test Results

3.1. Tunnel Failure Process. In order to observe the changes of surrounding rock during the tunneling of TBM tunnel, combing the real time change of the pressure and displacement of the surrounding rock, the tunnel morphology of different length of TBM tunneling was photographed and analyzed, as shown in Figure 7.

When TBM enters 22.5 cm, that is, the excavation faces do not reach the interface between the surrounding rock and the fault zone, the excavation faces have obvious tool scratches, the tunnel forming quality is good, and no surrounding rock falls off. When TBM enters 42.5 cm, that is, the excavation face of the hand has a small section of the fracture zone exposed, the arch of tunnel has significant deformation, the right arch of the shoulder of the fracture caused partial peeling, and the tunnel is relatively stable. When TBM enters 52.5 cm, half of the fracture zone material on the excavation faces are exposed, and a little arch roof falls off, and the fracture in the shoulder of the right arch develops rapidly, and the surrounding rock falls off, forming a small landslide near the interface of two different materials. When TBM enters 72.5 cm, that is, the excavation faces are all fracture zone material, the TBM cutter head enters the fracture zone as a whole, large deformation occurs in the surrounding rock tunnel above the excavation faces, the cave-in does not connect to the surface, the internal form is similar to that of a silo, the earth pressure box sensor falls, the cave-in ceiling is 51 cm, 1.46 D (D is tunnel diameter), and the tunnel is unstable. At the same time, the cave-in soil above the tunnel was immediately piled up in front of the cutter head, and the slag could not be removed in time, causing the TBM to jam.

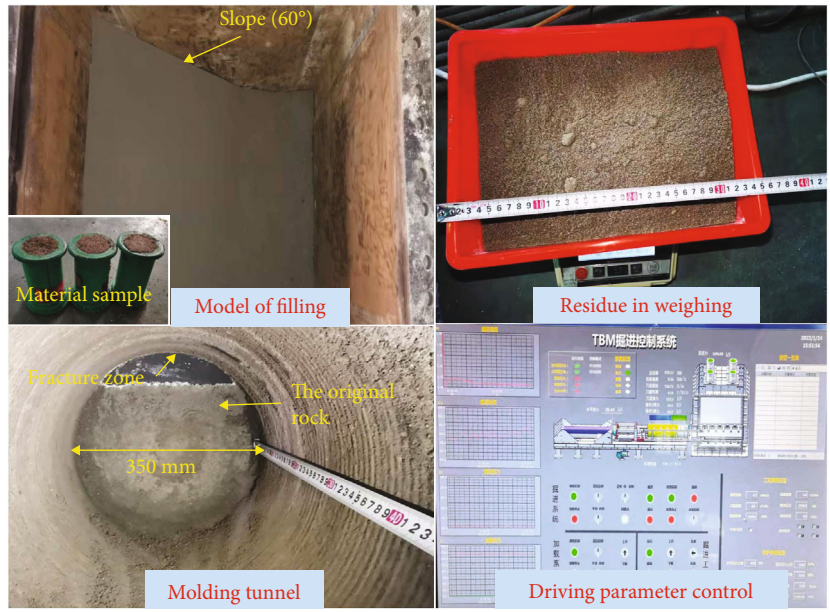

Figure 6: Miniature TBM driving test process.

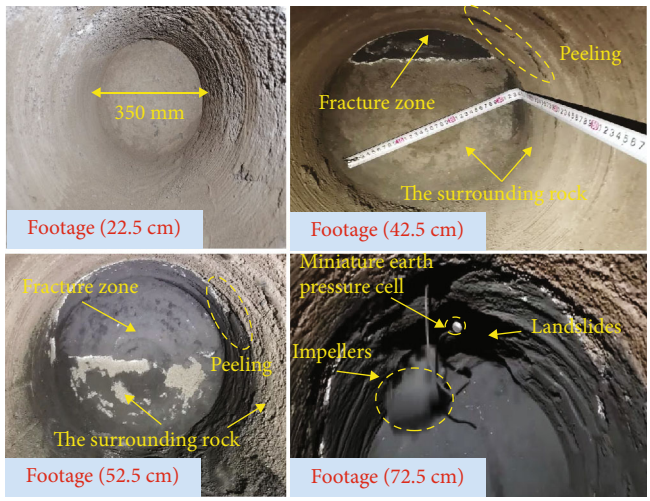

Figure 7: Tunnel shape diagram of micro TBM with different footage.

3.2. Surrounding Rock Pressure Change. Figures 8–10 show the variation curves of the pressure of surrounding rock above the tunnel with the distance driven by TBM.

This can be seen in Figure 8 that the surrounding rock pressure at E1 and E2 increases and then decreases as a whole. The E1 has a maximum of 66.91 kPa and a loaded ambient rock pressure of 56.22 kPa. The pressure of surrounding rock caused by TBM excavation disturbance increases is 1.19 times higher than before excavation. Similarly, the pressure of surrounding rock at E2 is 1.16 times higher than it was before the excavation. During the construction of TBM tunneling, there are three surrounding rock pressure drop zones. When TBM excavates 22.5 cm (zone I), there is slight congestion in the micro-TBM spiral slag hole, and when TBM retreats, the excavation faces lack thrust support, the surrounding rock pressure decreases, and the surrounding rock pressure increases after reexcavating. When TBM excavated into the second section, the pressure of the surrounding rock increased faster when excavating into the E1 pressure box. After removing slag, the pressure of the surrounding rock leveled off and reached the maximum. When TBM tunneling was excavated to 37.5 cm (fault interface), on-site rock pressure (E2) dropped sharply due to the slippage of loose material on the fault. When TBM tunneling is dug up to 42.5 cm, the rock pressure increased due to a combination of muck accumulation and thrust from the cutter head. The pressure on the surrounding rock of E1 began to fluctuate as TBM dug in at 10 cm (17.5 cm, that is, 0.5 D from E1). The pressure on the surrounding rock at E2 increased after excavating to 22.5 cm (15 cm, that is, 0.43 D from E2).

This can be seen in Figure 9. Surrounding rock pressure in E3, E4, and E5 presents an overall downward trend. When TBM tunneling reaches 42.5-62.5 cm, the stress fluctuation drops sharply and then tends to be stable. With the fracture zone inclination of 60°, the material of the fracture zone above the surface of the tunnel face increased from 1/3 to 2/3 when TBM tunnel was dug between 42.5 cm and 62.5 cm. At the same time, the surrounding rock below the E3 pressure box first appears loose; the surrounding rock above the tunnel is easy to creep into the tunnel, resulting in the release of surrounding rock pressure and resulting in a large loose under the E3 pressure box and a smaller loose area under the E5, where the pressure of the surrounding rock fell the most, from 42.46 kPa to 25.88 kPa, a decrease of about 39.05%. Surrounding rock pressure fell the least in E5 and decreased the least, by about 5.38 per cent. As a result, as TBM pushes into the fault zone, it is easy to cause the surrounding rocks on the fault to collapse and pile up and, in severe cases, to get stuck on the cutter head.

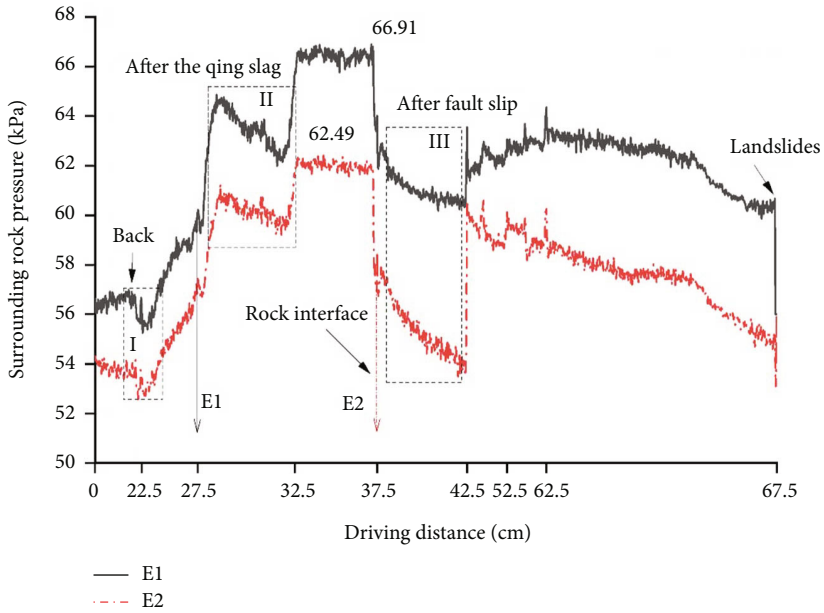

Figure 8: Pressure curves of surrounding rock at E1 and E2.

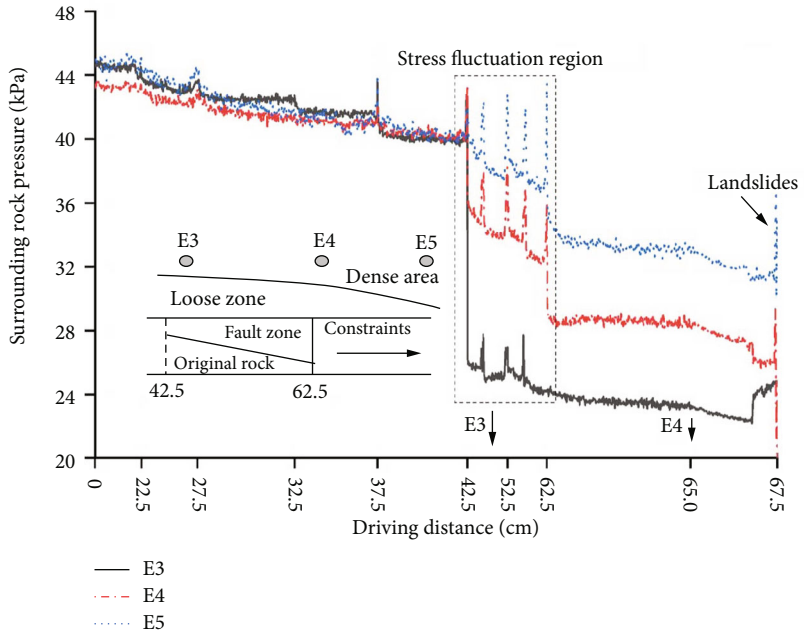

Figure 9: Surrounding rock pressure curves at E3, E4, and E5.

Figure 10 shows that the pressure of surrounding rocks in E6 to E9 varies little, with a maximum decrease of 5.23%. The overall trend is downward and can be divided into three stages: the first stage is a slow drop zone, mainly because the surrounding rock of the tunnel in front of the fracture zone interface is high and dense. The support to the surrounding rock in front of the tunnel decreases gradually after TBM excavation, and the pressure of surrounding rock decreases gradually at E6~E9. In the second stage, TBM gradually excavates to the fault zone, and the surrounding rock pressure is stable at E6~E9. After the tunnel collapse of the tunnel in the third stage, the support to the surrounding rock in front of the tunnel decreases, the pressure of surrounding rock decreases, and the pressure of surrounding rock stabilizes after the accumulation of the surrounding rock in front of the tunnel stabilizes. The distance from the E6 measurement point to the start of the fault zone is 1.73 times the length of horizontal projection (H) of the fault zone interface, that is, meaning that TBM has an impact the fault zone is 1.73 H in front of it.

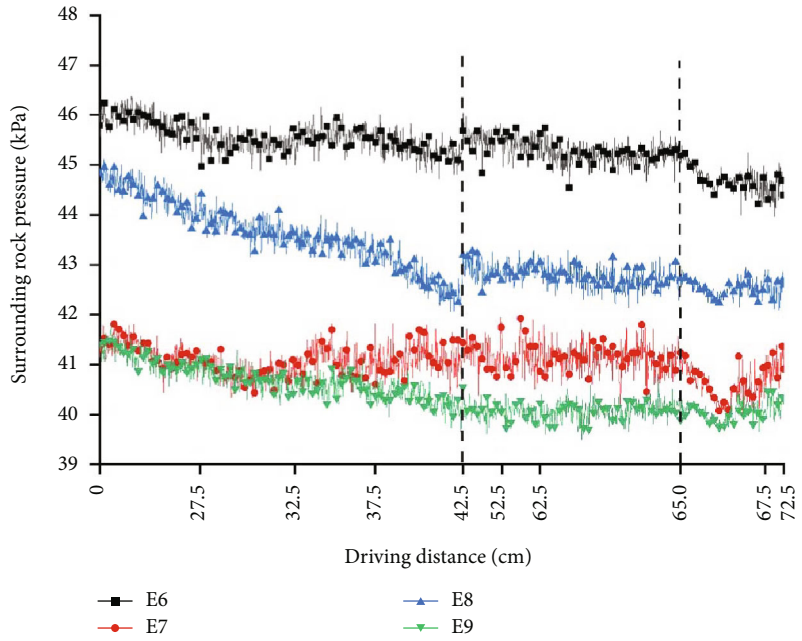

Figure 10: Pressure curves of surrounding rock from E6 to E9.

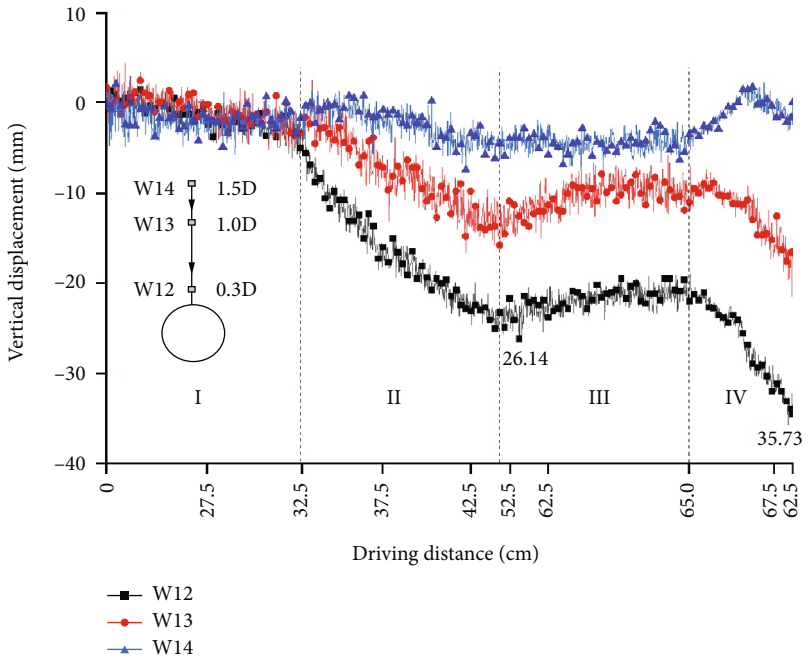

Figure 11: Vertical displacement curves of surrounding rock from W12 to W14.

3.3. Variation of Surrounding Rock Displacement. Figure 11 Internal displacement curve of surrounding rock above tunnel vault driven by TBM. As can be seen from the diagram, the internal displacement of the surrounding rock as a whole appears to have become a tunnel. The closer the tunnel contour, the greater the displacement, with a maximum displacement of 26.14 mm in the deformation phase and 35.73 mm in the vertical direction after the tunnel collapse. The vertical displacement curve of the surrounding rock has four stages: phase I is stable, with little change in displacement. The second stage is the displacement decline stage, W12, and W13 displacement decreases faster compared to W14. Surrounding rock displacement decreased to 32.5 cm after TBM tunnel excavation, that is, 1.21 D in front of the monitoring section, the reason for the surrounding rock displacement decline may have been caused by the internal surrounding rock loosening as the upper surrounding rock slides along the interface during the excavation of

the TBM tunnel to the fracture interface. In the third stage, the displacement of the surrounding rock increased slightly, mainly due to a decrease in the proportion of metacarpals to 52.5 cm of primary rock after excavation until all the TBM enters the fault zone, fault zone, a decrease in the range of fracture zone material sliding along the interface, and a reaction of loose material in front of the blade plate on the internal surrounding rock, causing the rise of the internal surrounding rock. In the fourth stage, the displacement of surrounding rock shows a downward trend. When tunnel collapse, the displacement of the surrounding rock drops precipitously. In addition, by comparing the displacement of the three points, it can be seen that the overall displacement of surrounding rock of W14 varies little, that is, the impact of the TBM excavation fault zone on the surrounding rock above the tunnel does not exceed 1.5 days.

3.4. Conclusions and Recommendations. In this paper, a 3D model similarity experiment is performed on a micro-TBM tunneling platform. The tunnel deformation and failure rule of TBM crossing large inclination fracture zone under high ground stress are studied. The main conclusions are as follows:

(1) Simulated experiments of TBM excavation in large inclination fracture zone under high ground stress are carried out by using TBM excavation test platform. Tunnels have good forming quality. TBM right arched shoulder cracks as it passes through the fracture interface. The vault collapsed silo style after all TBM cutters enter the fracture zone

(2) The maximum pressure of surrounding rock before TBM tunneling is 66.91 kPa, and the influence of TBM tunneling increases 1.19-fold. Surrounding rock pressure rises and then falls in the primary rock (below the interface), and precipitous decline occurs under the influence of sliding of surrounding rock above the interface of the fault zone. Impact range of TBM excavation is 0.43 D to 0.5 D before the head is cut. The pressure of surrounding rocks in the fault zone is generally decreasing. When the material content of the fault zone increases from 1/3 to 2/3, the pressure fluctuation due to the loose zone is caused by the sliding of the surrounding rock. When TBM passes through the fault zone interface, the pressure of surrounding rock at front edge does not affect the range greater than 1.73 H

(3) The displacement of surrounding rock above the tunnel vault has four distinct phases with TBM tunneling. The closer you get to the outline of the tunnel, the more displaced people. Surrounding rock displacement decreases the most when TBM crosses the fault zone interface. The TBM disturbance affects 1.21 d in front of the cutter head and no more than 1.5 d above the vault

(4) Through the analysis of the deformation law of surrounding rock pressure and displacement with the tunneling distance, it is found that tunneling has obvious influence on the stress and displacement of surrounding rock through the fault zone interface. Therefore, the interface of the fault zone should be strengthened in advance to reduce the construction risk before the construction of the span fault zone

Data Availability

The data used to support the findings of this study are available from the corresponding author upon request.

Conflicts of Interest

The authors declare that they have no conflicts of interest.

Authors' Contributions

Liming Wang and Kairong Hong are responsible for the conceptualization; Liming Wang, Hailei Zhao, Zhenxing Yang, and Zhenliang Zhou for the methodology; Liming Wang, Hailei Zhao, and Zhenxing Yang for the formal analysis and investigation; Liming Wang for the writing—original draft preparation; Hailei Zhao and Zhenxing Yang for the writing—review and editing; and Xiangbo Zhao for the funding acquisition. Liming Wang and Kairong Hong contributed equally to this work and should be considered co-first authors.

Acknowledgments

This work was supported by the National Key Research and Development Program of China (2020YFB2006804), Key Science and Technology of Henan Province (212102310270), National Natural Science Foundation of China (no. 52108365), Natural Science Foundation of Henan Province of China (no. 202300410001); Research Project of Xinjiang Ertysh River Basin Development And Construction Management Bureau (EQ076/FY057), and Science and Technology Innovation Plan of China Railway Tunnel Bureau Group (Suiyanhe 2019-10).

References

[1] K. R. Hong, "Innovation and practice of hard rock TBM in China," *Tunnel Construction*, vol. 38, no. 4, p. 519, 2018.

[2] Á. Tóth, Q. M. Gong, and J. Zhao, "Case studies of TBM tunneling performance in rock–soil interface mixed ground," *Tunnelling and Underground Space Technology*, vol. 38, pp. 140–150, 2013.

[3] L. J. Jing, N. Zhang, and C. Yang, "Development of TBM and its construction technologies in China," *Tunnel Construction*, vol. 36, no. 3, p. 331, 2016.

[4] K. R. Hong, "Development and thinking of tunnels and underground engineering in China in recent 2 years (from 2019 to 2020)," *Tunnel Construction*, vol. 41, no. 8, p. 1259, 2021.

[5] N. Barton, *Tunneling in Jointed and Faulted Rock*, A. A. Balkema, Ed., Rotterdam, The Netherlands, 2000.

[6] H. L. Zhao, K. Chen, J. J. Zhou, B. Zhang, B. Yang, and Z. F. Wang, "The research on construction technology of TBM

continuous through the limestone section of no. 4 bid of Songhua River water conveyance project," *Tunnel construction*, vol. 37, no. 3, p. 354, 2017.

[7] Y. J. Shang, Z. F. Yang, Q. L. Zeng, Y. C. Sun, Y. Y. Shi, and G. X. Yuan, "Retrospective analysis of TBM accidents from its poor flexibility to complicated geological conditions," *Chinese Journal of Rock Mechanics and Engineering*, vol. 26, no. 12, p. 2404, 2007.

[8] M. Khosravi, A. Ramezanzadeh, and S. Zare, "Effects of joint orientation and spacing on the boreability of jointed rock mass using tunnel boring machines," *Arabian Journal of Geosciences*, vol. 14, no. 1, p. 61, 2021.

[9] M. C. Villeneuve, "Hard rock tunnel boring machine penetration test as an indicator of chipping process efficiency," *Journal of Rock Mechanics and Geotechnical Engineering*, vol. 9, no. 4, pp. 611–622, 2017.

[10] R. Hasanpour, J. Rostami, J. Schmitt, Y. Ozcelik, and B. Sohrabian, "Prediction of TBM jamming risk in squeezing grounds using Bayesian and artificial neural networks," *Journal of Rock Mechanics and Geotechnical Engineering*, vol. 12, no. 1, pp. 21–31, 2020.

[11] C. Laughton, "Geotechnical problems encountered by tunnel boring machines mining in sedimentary rocks," in *Underground Space Use. Analysis of the Past and Lessons for the Future*, CRC Press, 2005.

[12] T. Shen, "Development of geomechanic model experiment techniques," *Journal of Yangtze River Scierntific Research Institute*, vol. 5, pp. 32–36, 2001.

[13] H. H. Shaalan, M. A. M. Ismail, and R. Azit, "Effect of tunnel overburden stress on the rock brittle failure depth," *Arabian Journal of Geosciences*, vol. 12, no. 4, p. 108, 2019.

[14] Q. Liu, C. J. Zhang, T. Y. Yan, J. H. Li, and C. S. Chen, "Analysis on interaction between rock and opened TBM during excavation in fault fracture zone: case of Xianglushan tunnel in Central Yunnan water diversion project," *Yangtze River*, vol. 52, no. 10, pp. 165–175, 2021.

[15] M. Maleki and R. Dehnavi, "Influence of discontinuities on the squeezing intensity in high insitu stresses (a tunnelling case study; actual evidences and TBM release techniques)," *Rock Mechanics and Rock Engineering*, vol. 11, pp. 1–23, 2018.

[16] C. Jian-long, Y. A. Sheng-qi, L. I. Xue-hua, P. Yu-cong, Z. Weisheng, and T. Wen-ling, "Impact of longitudinal displacement profile relaxation on contract force acted on double shield TBM in squeezing ground," *Rock and Soil Mechanics*, vol. 37, no. 5, pp. 1399–1407, 2016.

[17] H. Chakeri, R. Hasanpour, M. A. Hindistan, and B. Ünver, "Analysis of interaction between tunnels in soft ground by 3D numerical modeling," *Bulletin of Engineering Geology and the Environment*, vol. 70, no. 3, pp. 439–448, 2011.

[18] R. Hasanpour, H. Chakeri, Y. Özcelik, and H. Denek, "Evaluation of surface settlements in the Istanbul metro in terms of analytical, numerical and direct measurements," *Bulletin of Engineering Geology and Environment*, vol. 71, no. 3, pp. 499–510, 2012.

[19] A. Lambrughi, L. Medina Rodríguez, and R. Castellanza, "Development and validation of a 3D numerical model for TBM-EPB mechanised excavations," *Computers and Geotechnics*, vol. 40, pp. 97–113, 2012.

[20] K. Arora, M. Gutierrez, and A. Hedayat, "Physical model simulation of rock-support interaction for the tunnel in squeezing ground," *Journal of Rock Mechanics and Geotechnical Engineering*, vol. 14, no. 1, pp. 82–92, 2022.

[21] S. Jeon, J. Kim, Y. Seo, and C. Hong, "Effect of a fault and weak plane on the stability of a tunnel in rock—a scaled model test and numerical analysis," *International Journal of Rock Mechanics and Mining Sciences*, vol. 41, pp. 658–663, 2004.

[22] Q. S. Zhang, D. M. Wang, S. C. Li, X. Zhang, Y. H. Tan, and K. Wang, "Development and application of model test system for inrush of water and mud of tunnel in fault rupture zone," *Chinese Journal of Geotechnical Engineering*, vol. 39, no. 3, pp. 417–426, 2017.

[23] W. S. Zhu, Y. Li, L. Zhang et al., "Geomechanical model test on stability of cavern group under high geostress," *Chinese Journal of Rock Mechanics and Engineering*, vol. 27, no. 7, pp. 1308–1314, 2008.

[24] L. I. Shu-chen, M. A. Teng-fei, and Y. J. Jiang, "Model tests on deformation and failure laws in excavation of deep rock mass with multiple fracture sets," *Chinese Journal of Geotechnical Engineering*, vol. 38, no. 6, pp. 987–995, 2016.

[25] B. Ghabraie, G. Ren, and J. V. Smith, "Characterising the multi-seam subsidence due to varying mining configuration, insights from physical modelling," *International Journal of Rock Mechanics and Mining Sciences*, vol. 93, pp. 269–279, 2017.

[26] M. L. Huang, F. Xu, and Z. Y. Wu, "Monitoring and analysis of influence of tbm construction on surrounding rock stability under urban environment and supporting parameters optimization," *Chinese Journal of Rock Mechanics and Engineering*, vol. 31, no. 7, pp. 325–1333, 2012.

[27] X. B. Zhao, L. M. Wang, J. Wang, and H. L. Zhao, "Research on mechanical performance of TBM tunnel supporting structure based on field test," *Henan Science*, vol. 40, no. 1, pp. 54–58, 2022.